Noise in Short Channel MOSFETs

John A. McNeill
Department of Electrical and Computer Engineering
Worcester Polytechnic Institute
Worcester, MA 01609
e-mail: mcneill@ece.wpi.edu

***Abstract*—For long-channel MOSFETs, the power spectral density of wideband noise in the drain current is predicted by an expression derived from thermal noise in the MOSFET channel. For short channel MOSFETs, observed noise can be much higher than predicted from thermal noise analysis of long channel MOSFETs. While the cause of this excess noise is the subject of some controversy, it can be understood by considering the fundamental difference between shot noise (carrier motions are independent events) and thermal noise (carrier motions are dependent due to thermal equilibration). This paper reviews the literature on noise in short channel MOSFETs and shows that the increased noise can be seen as resulting from the current noise approaching a shot noise limit as carrier transit time in the MOSFET channel becomes so small that thermal equilibration does not have time to occur.**

***Index Terms* - Thermal noise, shot noise, device noise.**

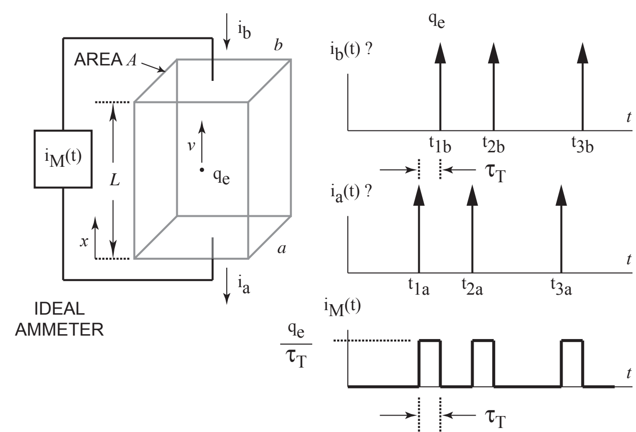

Fig. 1. Idealized physical configuration for analyzing shot noise.

I. Introduction

Designers of analog and mixed-signal integrated circuits face both challenges and opportunities as CMOS device dimensions enter the nanoscale region. For mixed-signal design, scaling offers the possibility of increased speed but also difficulties associated with reduced supply voltage, degraded transistor characteristics, and increased variability. An additional issue in short channel devices is an increase in wideband noise over the noise observed in long-channel devices.

The purpose of this paper is to review fundamental noise sources of interest to circuit designers, bringing in some results from statistical physics that may be less familiar to design engineers. Sections II and III review shot noise and thermal noise, respectively. The insights from each of these types of noise are applied to the MOSFET in section IV.

II. Shot Noise

Figure 1 shows an idealized physical configuration for analyzing shot noise. Consider a volume defined by two conductive plates a and b with area A separated by a distance L. At random times $t_{1a}, t_{2a}, \ldots$ an electron leaves plate a and travels at constant velocity v in the positive x direction toward plate b, arriving after a transit time delay τ_T at plate b at times $t_{1b}, t_{2b}, \ldots$. The situation is roughly analogous to the collection of carriers at the reverse-biased base-collector junction of a bipolar transistor [1], [2] or the motion of carriers in a vacuum tube [3]–[5]. The key idealization is that current flows in discrete charges which undergo only a transit time delay, and are not scattered or otherwise impeded by interaction with any medium or with other carriers. [1]

We now consider the question: What current $i_M(t)$ would be measured by an ideal ammeter connected in series with this volume, as shown in Fig. 1? Considering only the passage of charge at plate a, one is tempted to say that the current $i_a(t)$ would be a series of impulses, with area equal to the electron charge q_e, at times $t_{1a}, t_{2a}, \ldots$, and that this must be the current $i_M(t)$. However, applying the same argument at plate b gives a different current $i_b(t)$. Which is correct?

A. Ramo-Shockley Theorem

The resolution of this apparent paradox is provided by the Ramo-Shockley theorem [3], [4], which states that the current measured in an external conductor from a charge q_e moving at velocity v between large ($A \gg L^2$) plates separated by a distance L is given by

$$i = \frac{q_e v}{L} \tag{1}$$

The reason that the external ammeter "knows" about the electron in transit between the plates is that the electric field on the plates is changing as the electron is moving. The changing electric field produces a displacement current which constitutes the external $i_M(t)$ while the electron is in motion.

[1]The cases of nonuniform velocity and interaction between carriers can be addressed using the techniques of [3]–[5]

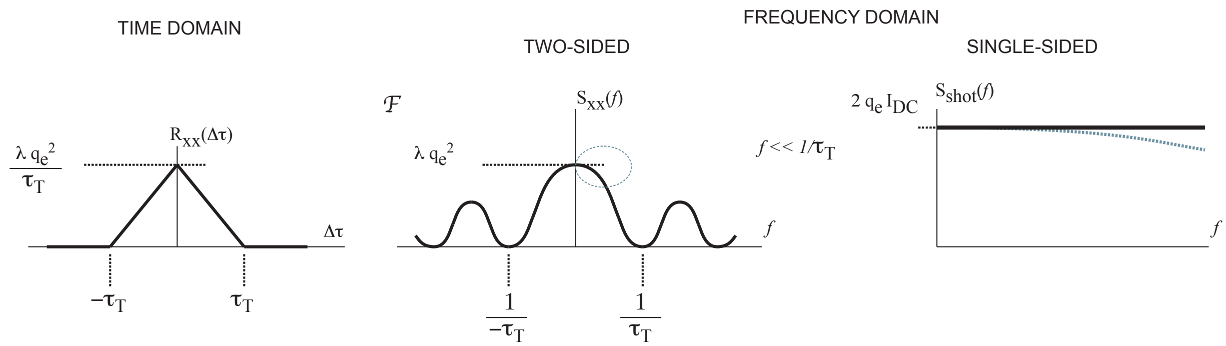

Fig. 2. Shot noise (a) autocorrelation, (b) Two-sided p.s.d., and (c) single-sided p.s.d. for frequencies $f \ll 1/\tau_T$.

Since the transit time τ_T is related to the velocity and distance by $v = L/\tau_T$, we can rewrite (1) as

$$i = \frac{q_e}{\tau_T} \tag{2}$$

which is shown for $i_M(t)$ in Fig. 1.

B. Noise Description

The current $i_M(t)$ can be described as an average DC value plus a random component due to the random occurrences of the charge carrying events. To describe the situation accurately, we need to be more precise about the "random" times $t_{1a}, t_{2a}, \ldots$ referred to in Fig. 1. For the Poisson random process [6], [7], the electron transits are independent events characterized by a parameter λ, which has units of 1/time, and is the expected number of arrivals per unit time. For long intervals of time $\Delta T \gg 1/\lambda$, the number of arrivals $N_{\Delta T}$ has an expected average value $E[N_{\Delta T}]$ given by

$$E[N_{\Delta T}] = \lambda \Delta T \tag{3}$$

and for short intervals of time $\delta t \ll 1/\lambda$, the probability of an electron arrival occurring is given by

$$P\{\text{electron in } \delta t\} = \lambda \delta t \tag{4}$$

To determine the average current I_{DC} over an interval of time ΔT, we use (3) in the definition of DC current $I_{DC} = \Delta Q/\Delta T$, where ΔQ is the average amount of charge transferred in time interval ΔT:

$$I_{DC} = \frac{\Delta Q}{\Delta T} = \frac{q_e N_{\Delta T}}{\Delta T} = \frac{q_e \lambda \Delta T}{\Delta T} = \lambda q_e \tag{5}$$

To describe the random component of $i_M(t)$, we may work in either the time domain (autocorrelation) or the frequency domain (power spectral density). For the waveform of Fig. 1, the autocorrelation [6], [8] is as shown in Fig. 2a.

By the Wiener-Khinchine theorem [6], [7], the Fourier transform of the autocorrelation gives the two-sided power spectral density (p.s.d.)

$$S_{xx}(f) = \lambda q_e^2 \frac{sin^2(\pi f \tau_T)}{(\pi f \tau_T)^2} \tag{6}$$

which is shown in Fig. 2b.

For frequencies $f \ll 1/\tau_T$, the power spectral density approaches a constant value λq_e^2. Converting to a single-sided power spectral density and substituting for the DC current from (5) gives a shot noise power spectral density

$$S_{shot}(f) = 2 q_e I_{DC} \tag{7}$$

which is shown in Fig. 2c. The assumption of "white" (independent of frequency) power spectral density is valid for frequencies $f \ll 1/\tau_T$.

Some points to notice:

- The discrete nature of charge is essential
- The carrier transits are independent events
- The charge carrying particles do not interact with each other or with any medium
- Temperature does not enter into the analysis at all

III. Thermal Noise

Figure 3a shows an idealized physical configuration for analyzing thermal noise. Consider a volume defined by two conductive plates a and b with area A separated by a distance L. The enclosed volume is filled with many electrons, with an average carrier concentration of n mobile electrons per unit volume. Unlike the case of Fig. 1, the carriers undergo scattering collisions, exchanging energy and momentum with the medium. The situation is roughly analogous to the motion of carriers in a semiconductor or resistor [1].

As the carriers move about due to random thermal motion, the ideal external ammeter will measure a current $i_M(t)$. What are the statistical properties of the current $i_M(t)$?

Note that resistor thermal noise can be explained without any reference to individual charge carriers; for example, Nyquist's original paper [9] derives the thermal noise density from considering modes of energy storage on an ideal transmission line. In this section we explicitly consider the motion of carriers to re-derive the thermal noise expression from fundamental principles of thermodynamics.

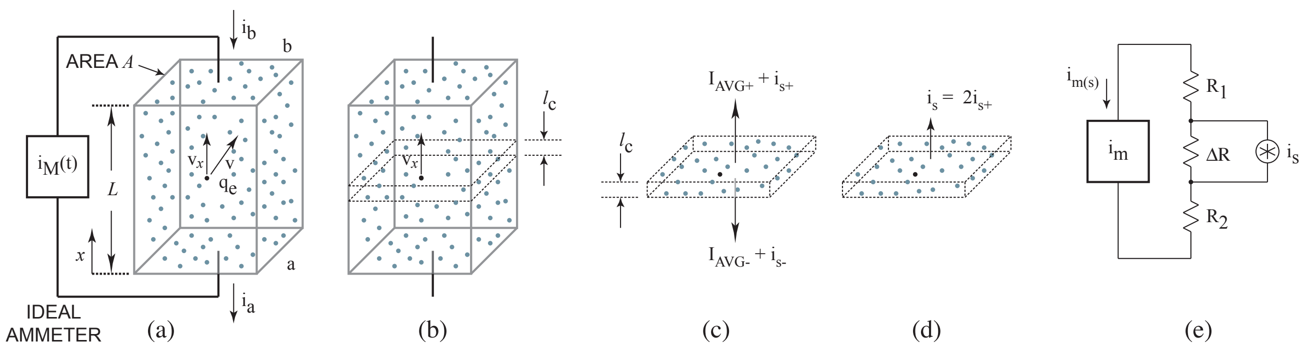

Fig. 3. (a) Idealized physical configuration for analyzing thermal noise, (b) "slice" of length l_c equal to mean free path, (c) average and varying components of current exiting each side of slice, (d) net current contributed by slice, and (e) contribution tot total current affected by current divider equivalent network.

A. Thermodynamics: Equipartition Principle

According to the equipartition theorem of thermodynamics [9], for a system in thermodynamic equilibrium, each independent energy storage mode will have an average energy of $kT/2$, in which Boltzmann's constant $k = 1.38066 \times 10^{-23} J/K$ and T is absolute temperature. For the electrons in Fig. 3, the velocity vector $\mathbf{x}$ can in general point in any direction; each component in the x, y, and z directions represents an independent energy storage mode in the kinetic energy of the electron. Since only the v_x component will contribute to the external current $i_M(t)$, we consider only v_x. By the equipartition principle, we equate the average kinetic energy in the x direction to the thermal energy of $kT/2$:

$$\frac{1}{2} m_n v_x^2 = \frac{1}{2} kT \tag{8}$$

$$v_x^2 = \frac{kT}{m_n} \tag{9}$$

using the effective mass m_n so we can treat the electron as a classical particle. At $T = 300K$, m_n for conductivity of electrons in silicon is

$$m_n = 0.26 m_0 \tag{10}$$

where $m_0 = 0.91094 \times 10^{-34} kg$ is the electron rest mass [1].

At $T = 300K$ we have

$$v_x^2 = \frac{(1.38066 \times 10^{-23} J/K)(300K)}{0.26(0.91094 \times 10^{-30} kg)} \tag{11}$$

$$v_x^2 \approx (1.0 \times 10^7 cm/sec)^2 \approx (0.1 \mu m/psec)^2 \tag{12}$$

As the electron wanders around through the medium, it undergoes collisions and is randomly scattered. Adopting the nomenclature of [1], the average time between collisions is called the "mean free time" τ_c and the average distance between collisions is called the "mean free path" l_c. The average velocity can be used to relate the mean free path and the mean free time τ_c:

$$v_x^2 = \frac{l_c^2}{\tau_c^2} \tag{13}$$

Typical values for a semiconductor are of order 1psec for τ_c and $0.1\mu m$ for l_c [1].

B. Derivation of Thermal Noise

To derive an expression for thermal noise density in the system of Fig. 3a, we subdivide the volume into "slices" of length l_c along the x-axis as shown in Fig. 3b. Assuming an average uniform carrier concentration of n carriers per unit volume, the number of carriers in the slice is given by

$$N_c = nAl_c \tag{14}$$

Adopting an approach similar to that of [10], we assume that during one mean free time τ_c, on average half of these carriers will exit this volume in the positive-x direction, and half will exit in the opposite direction. Thus the average currents I_{AVG+} and I_{AVG-} are equal in magnitude and opposite in sign, and using (14) are given by

$$I_{AVG+} = I_{AVG-} = q_e \frac{N_c/2}{\tau_c} = \frac{q_e n A l_c}{2\tau_c} \tag{15}$$

Note that this is only the average behavior; due to the random nature of the individual carrier velocities, each of the currents will have a shot noise component i_{s+} and i_{s-} as shown in Fig. 3c. Applying (7) to (15) gives for the shot noise p.s.d.

$$i_{s+}^2 = 2q_e I_{AVG+} = \frac{q_e^2 n A l_c}{\tau_c} \tag{16}$$

Note that $i_{s-} = -i_{s+}$, since every electron that does not exit one side must exit the other side. Thus the net current contributed by the slice is $i_s = 2i_{s+}$ as shown in Fig. 3d. The total shot noise densities add in correlated fashion

$$i_s^2 = 4i_{s+}^2 = \frac{4q_e^2 n A l_c}{\tau_c} \tag{17}$$

This is the p.s.d. of the current fluctuation in the slice with resistance ΔR; however, only a fraction of this current variation will be seen at the ideal ammeter in the p.s.d. $i_{m(s)}$ due to the current divider between ΔR (the resistance of the slice) and resistances R_1 and R_2 (the resistances of the material above and below the slice). The total resistance is $R = R_1 + \Delta R + R_2$; in the limit as $\Delta R \ll R$

$$i_m = \frac{\Delta R}{R} i_s \tag{18}$$

The current divider fraction $\Delta R/R$ is related to the lengths l_c and L by

$$\frac{\Delta R}{R} = \frac{l_c}{L} \tag{19}$$

so using (19) and (17) in (18) gives the contribution of the ΔR slice to the current noise density seen at $i_m(s)$ as

$$i^2_{m(s)} = \left(\frac{l_c}{L}\right)^2 \frac{4q_e^2 nAl_c}{\tau_c} \tag{20}$$

The contributions from each "slice" are independent and will add in uncorrelated fashion. Since there are a total of L/l_c slices, the total current noise density seen by i_m will be

$$i^2_m = \left(\frac{L}{l_c}\right)\left(\frac{l_c}{L}\right)^2 \frac{4q_e^2 nAl_c^2}{L\tau_c} \tag{21}$$

To put (21) in a form that relates to the total resistance R, we first multiply the numerator and denominator by τ_c:

$$i^2_m = \frac{4q_e^2 nA\tau_c l_c^2}{L\tau_c^2} \tag{22}$$

From (8) and (13) we have

$$\frac{l_c^2}{\tau_c^2} = v_x^2 = \frac{kT}{m_n} \tag{23}$$

Substituting from (23) into (22) gives

$$i^2_m = \frac{4q_e^2 nA\tau_c kT}{Lm_n} \tag{24}$$

In [1], it is shown that the mobility μ is given by

$$\mu = \frac{q_e\tau_c}{m_n} \tag{25}$$

Substituting (25) into (24) gives

$$i^2_m = \frac{4q_e n\mu AkT}{L} \tag{26}$$

In [1], it is also shown that the the resistance of the structure in Fig. 3a is given by

$$R = \frac{L}{q_e n\mu A} \tag{27}$$

Substituting (27) into (26) gives

$$i^2_m = \frac{4kT}{R} = S_{thermal}(f) \tag{28}$$

which is the familiar result for wideband thermal noise of a resistor. In this case, with analogy to (6) and (7), the white p.s.d. assumption is valid for frequencies $f \ll 1/\tau_c$.

Some points to notice:

- The individual behavior of carriers is not essential to thermal noise; behavior is described by the aggregate result of many carrier motions
- The charge carrying particles interact with the medium in a dissipative manner through scattering, and thereby are in thermal equilibrium
- Temperature is important in the analysis, determining the average kinetic energy of the carriers

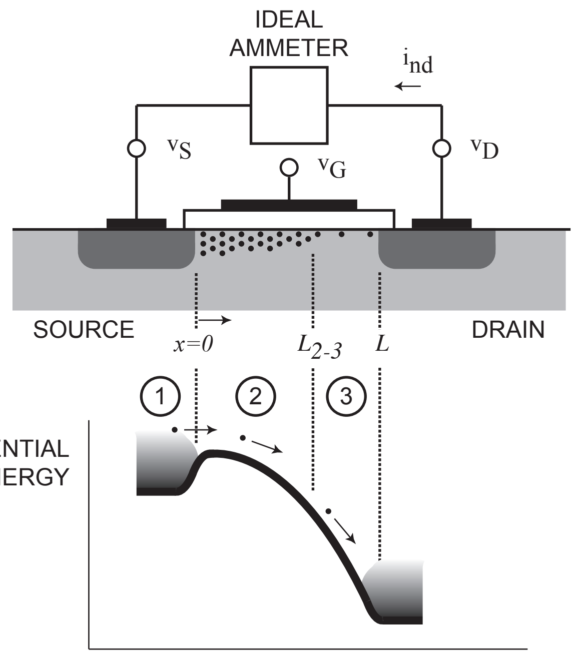

Fig. 4. Carrier flow, potential energy for general MOSFET.

IV. Noise in MOSFETs

Figure 4 shows a conceptual view of an n-channel MOSFET, operating in saturation. A cross-sectional view of the channel is shown, with inversion layer between the source and drain formed by the gate voltage v_G. Also shown is a conceptual plot of the electron potential energy along the source-drain channel [11], [12]. We consider only effects relevant to wideband drain current noise, not 1/f noise or induced gate noise [11]. Although we will consider velocity saturation, we will neglect the carrier multiplication role of "hot" electrons since the effect on wideband noise is not significant [13], [14].

As described in [1], [10]–[12] there are three types of carrier motion as an electron moves from source to drain:

1) Injection over potential barrier into channel: For a carrier to enter the source-drain channel, it must have enough energy to overcome the potential barrier (shown in Fig. 4 at $x = 0$) at the source-channel p-n junction. The height of the barrier depends on several factors including the potential profile in the channel as well as other dimensional effects not represented in the simple picture of Fig. 4.
2) Low field motion according to drift: At the source end of the channel ($0 < x < L_{2-3}$), the x-direction component of the electric field is below the critical value at which velocity saturation occurs [1], [11]. The

carrier undergoes scattering collisions and exchanges energy with the lattice, is in thermal equilibrium with its environment, and its average velocity is adequately described by the mobility relationship. In this region, the thermal noise relationships of section III apply.

3) High field motion with velocity saturation: At the drain end of the channel ($L_{2-3} < x < L$) the x-direction component of the electric field exceeds its critical value and velocity saturation occurs.

As described in [13], [14], [16], carrier motion in the velocity saturated region (3) will not contribute appreciably to noise: since the velocity is limited to v_{sat}, the carriers do not respond to any external influence and the statistics of carrier arrival at the drain are determined by behavior in regions (1) and (2).

A. Regions of MOSFET Drain Current Noise

A key consideration in understanding drain current noise for the MOSFET in saturation is the size of the L_{2-3} length relative to the mean free path l_c:

1) $L_{2-3} \gg l_c$: If the low-field region of the channel is long compared to the mean free path l_c, then noise is analyzed by breaking the inversion layer into small segments, treating each as a resistor with thermal noise, and integrating to obtain the total noise of the drain current [15]. In saturation,

$$i_{nd}^2 = 4\gamma kT g_m \tag{29}$$

where the factor $\gamma = 2/3$ for the long channel case results from the integration over the channel length and takes into account the influence of the gate voltage on charge density and carrier motion in the inversion layer. A key assumption underlying the derivation of (29) is that the carriers are behaving in resistive fashion. When this is not the case, it makes sense that observed noise behavior will deviate from the prediction of (29).

2) $L_{2-3} \leq l_c$: If the low-field region of the channel is short compared to the mean free path l_c, then the assumptions underlying (29) are not valid: Most carriers will not undergo any scattering collisions, the carriers are not in the channel for a sufficient time to reach thermal equilibrium, and carrier behavior will tend more toward the shot noise case described in section II. Depending on the statistics of carrier entry at (1) in Fig. 4, the drain current may show full shot noise as is known to occur in weak inversion operation [10], [11] or the shot noise may be partially suppressed [5], [18].

B. Analogy for Shot Noise Suppression

Figure 5 shows an analogy to consider for understanding the concept of shot noise suppression. Figure 5a shows a bipolar transistor with fixed v_{BE} bias. The output current noise i_{no}^2 will show the full shot noise i_{nc}^2 of the collector current, as carriers are randomly injected from the emitter into the base and then swept into the collector [2]. Figure 5b shows a bipolar transistor with emitter degneration. We assume the base voltage bias v_{B2} is adjusted to maintain the same DC collector current. With BJT transconductance g_m, small-signal

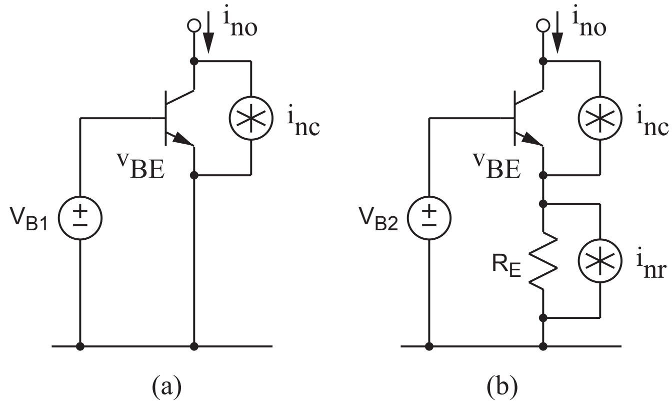

Fig. 5. Analogy for shot noise suppression: (a) BJT with fixed bias (b) BJT with emitter degeneration.

analysis for this case shows that the output current noise is given by

$$i_{no}^2 = \left(\frac{1}{1+g_m R_E}\right)^2 i_{nc}^2 + \left(\frac{g_m R_E}{1+g_m R_E}\right)^2 i_{nr}^2 \tag{30}$$

showing that the collector current shot noise component i_{nc} is suppressed by a factor $1/(1+g_m R_E)$. Intuitively, this suppression comes about through the negative feedback provided by the degeneration resistor: If there are (randomly) more carrier injections due to shot noise and the transistor current increases, the voltage drop across R_E increases, reducing v_{BE}, reducing the probability of future injection events and counteracting the current increase. As can be seen from (30), larger R_E provides more feedback and greater suppression of shot noise.

The analogous processes in the MOSFET are the injection of carriers from the source into the channel at (1) in Fig. 4, and the interaction of the carriers in the resistive portion of the channel at (2) in Fig. 4. As described in [18], if the carriers are in the resistive portion of the channel for an appreciable time, their interaction affects the potential profile of the channel shown in Fig. 4, and the probability of future carrier injections will be affected in a way that suppresses the randomness of carrier injection from the source. If the carriers are in the channel for a short period of time, and do not interact with the medium in resistive fashion, they will have a negligible effect on the potential profile shown in Fig. 4. Future carrier injections will tend to be independent events, leading to shot noise limited behavior. Indeed, as described in [18], the situation is similar to the ballistic MOSFET [12], [17] in which device operation is determined mainly by the injection of carriers from the source across the source-channel potential barrier.

V. Conclusion

Noise density expressions were derived from fundamental considerations for shot noise and thermal noise. In general, shot noise is associated with current flow in the form of carrier motion as individual independent events, whereas thermal noise in a resistive medium is associated with carrier interaction through scattering collisions and thermal equilibrium. The key assumptions underlying derivation of noise for long-channel MOSFETs are related to to the resistive behavior of carriers; however, these assumptions are violated in a MOSFET when carrier velocity approaches thermal velocity, effective channel length is less than the mean free path typically covered between scattering collisions, or carrier transit time is less than the time required for thermal equilibration. In these cases observed drain noise current density is greater than the thermal noise prediction, increasing toward a limiting value set by shot noise.

ACKNOWLEDGMENT

The author thanks Prof. David Cyganski of the WPI ECE department for valuable discussions.

REFERENCES

[1] S. M. Sze, "Semiconductor Devices: Physics and Technology." New York: Wiley, 2002.

[2] P. R. Gray, P. J. Hurst, S. H. Lewis, and R. G. Meyer, "Analysis and Design of Analog Integrated Circuits." New York: Wiley, 2008.

[3] S. Ramo, "Currents Induced by Electron Motion," *Proc. IRE*, pp. 584-585, Sept. 1939.

[4] W. Shockley, "Currents to Conductors Induced by a Moving Point Charge," *J. Applied Physics*, pp. 635-636, Oct. 1938.

[5] B. J. Thompson, D. O. North, and W. A. Harris, "Fluctuations in space-charge-limited currents at moderately high frequencies," *Electron Tubes, RCA Review*, vol. 1 (1935-41), pp. 58-160.

[6] K. S. Shanmugan and A. M. Breipohl, "Random Signals." New York: Wiley, 1988.

[7] R. D. Yates and D. J. Goodman, "Probability and Stochastic Processes." New York: Wiley, 1998.

[8] J. A. McNeill and D. R. Ricketts, "Designer's Guide to Jitter in Ring Oscillators." Springer, 2009.

[9] H. Nyquist, "Thermal agitation of electric charge in conductors," *Physical Review*, vol. 32, pp. 110-113, July, 1928.

[10] R. Sarpeshkar, T. Delbruck, and C. Mead, "White Noise in MOS Transistors and Resistors," *IEEE Circuits and Devices Magazine*, pp. 23-29, Nov. 1993.

[11] Y. Tsividis, "Operation and Modeling of the MOS Transistor." New York: McGraw-Hill, 1987.

[12] K. Natori, "Compact modeling of ballistic nanowire MOSFETs," *IEEE Trans. Electron Device*, pp. 2877-2885, Nov. 2008.

[13] K. Han, H. Shin, K. Lee, "Analytical drain thermal noise current model valid for deep submicron MOSFETs," *IEEE Trans. Electron Device*, pp. 261-269, Feb. 2004.

[14] M. J. Deen and C.-H. Chen, "MOSFET modeling for low noise, RF circuit design," *Proc. CICC*, pp. 201-208, Sept. 2002.

[15] A. van der Ziel, "Noise in Solid-State Devices and Circuits." New York: Wiley, 1986.

[16] A. J. Scholten, L. F. Tiemeijer, R. van Langevelde, R. J. Havens, A. T. A. Zegers-vanDuijnhoven, and V. C. Venezia, "Noise modeling for RF CMOS circuit simulation," *IEEE Trans. Electron Device*, pp. 618-632, March 2003.

[17] A. Rahman, J. Guo, S. Datta, M. S. Lundstrom, "Theory of ballistic nanotransistors," *IEEE Trans. Electron Device*, vol. ED-50, pp. 1853-1864, Sept. 2003.

[18] R. Navid, T. H. Lee, and R. W. Dutton, "A circuit-based noise parameter extraction technique for MOSFETs," *Proc. ISCAS*, pp. 3347-3350, May 2007.